

**Microscopic mechanisms of dephasing due to electron-electron interactions**

R. Žitko and J. Bonča

*FMF, University of Ljubljana, and J. Stefan Institute, Ljubljana, Slovenia*

(Received 18 September 2002; revised manuscript received 3 April 2003; published 13 August 2003)

We develop a nonperturbative numerical method to study tunneling of a single electron through an Aharonov-Bohm ring where several strongly interacting electrons are bound. Inelastic processes and spin-flip scattering are taken into account. The method is applied to study microscopic mechanisms of dephasing in a nontrivial model. We show that the electron-electron interactions described by the Hubbard Hamiltonian lead to strong dephasing: the transmission probability at flux  $\Phi = \pi$  is high even at small interaction strength. In addition to inelastic scattering, we identify two energy-conserving mechanisms of dephasing: symmetry-changing and spin-flip scattering. The many-electron state on the ring determines which of these mechanisms will be at play: transmitted current can occur either in elastic or inelastic channels, with or without changing the spin of the scattering electron.

DOI: 10.1103/PhysRevB.68.085313

PACS number(s): 73.63.-b, 71.10.-w, 72.10.-d

**I. INTRODUCTION**

Advances in the semiconductor technology made it possible to study quantum interference effects in mesoscopic systems where the wave nature of electrons plays an essential role. Particularly noteworthy are the studies of the Aharonov-Bohm (AB) oscillations in mesoscopic rings.<sup>1-3</sup> The analysis of results in terms of the single-electron picture turned out to be inadequate to describe the totality of phenomena. Inelastic scattering of electrons is believed to be the predominant mechanism responsible for the loss of the phase coherence in such experiments and the suppression of the  $h/e$  oscillations. When an electron interacts with optical phonons, the dephasing only occurs through inelastic processes.<sup>4</sup> At low temperatures the phonon degrees of freedom freeze out, therefore other mechanisms for dephasing should be taken into account. Measurements of the dephasing time saturation at low temperatures<sup>5,6</sup> show that zero-point fluctuations of the electromagnetic environment<sup>7</sup> could play a role in explaining this anomalous behavior. It is nevertheless believed that at low temperatures the electron-electron interaction is the dominant mechanism for dephasing.<sup>8,9</sup> Further support for the importance of electron correlations at very low temperatures comes from recent measurements of anomalous temperature dependence of the dephasing time in mesoscopic Kondo wires<sup>10</sup> where non-Fermi-liquid behavior has been found below the Kondo temperature.

The AB geometries have been theoretically studied using self-consistent mean-field approximations that break down for degenerate levels, which physically happens at very low temperatures.<sup>11-13</sup> The mean-field approximation does not describe transitions in which the symmetry of the many-electron wave function of correlated bound electrons changes, and it is thus inadequate to study dephasing. Keldysh-type Green's functions and numerical renormalization-group techniques<sup>14,15</sup> or equation of motion method<sup>16</sup> have been applied to AB systems, where calculations were limited to interacting quantum dot with two levels coupled to reservoirs. Particular attention was devoted to the appearance of the Kondo physics induced by changing the

magnetic flux, however, no spin-flip-induced dephasing has been investigated by these methods. A study of a Coulomb blockade regime was recently done by Xiong and Xiong<sup>17</sup> with a method similar to the one proposed in the present work. Their Hamiltonian, however, maps on a noninteracting model in the limit when the coupling to the leads is zero. Furthermore, they have only investigated spinless fermions and neglected inelastic scattering channels. Transmission of two interacting electrons was recently studied on the basis of continuous two-particle Hamiltonian, where an enhancement of transmission with increasing interaction strength was found.<sup>18</sup>

To shed some further light on the problem of dephasing in electron-tunneling experiments, there is obviously a demand for a capable method that would treat the problem of the scattering of an electron through a finite region where electron-electron ( $e-e$ ) interactions would be exactly taken into account. Such a method should be based on the use of exact correlated many-electron wave functions.

In this paper we propose a method that treats the  $e-e$  interactions by direct diagonalization of the many-body Hamiltonian using iterative (Lanczos) technique. The method naturally takes into account spin-flip processes, so it can predict the ratio of spin-flip over normal scattering processes. This makes the technique interesting for calculating spin-polarized transport<sup>19</sup> in the field of spintronics.

We apply the method to study single-electron transmission through an AB ring with  $e-e$  interactions. As is widely known, an electron perfectly reflects from an AB ring when the flux  $\Phi$  penetrating the ring is such that the phases gained by the electron traveling through the lower or the upper arm of the AB ring cancel ( $\Phi = \pi$ ). Such reflection occurs for any energy of the incident electron. This remains true even when there are electrons bound on the AB ring, as long as the system remains noninteracting. The main purpose of our investigation is in the influence of the finite Coulomb repulsion on the transmission of the electron in the case described above. We choose the Hubbard model to describe the AB ring. The Hubbard model is the simplest and yet the most important nontrivial prototype model for correlated electrons in the solid state. As we will show, finite Coulomb interac-

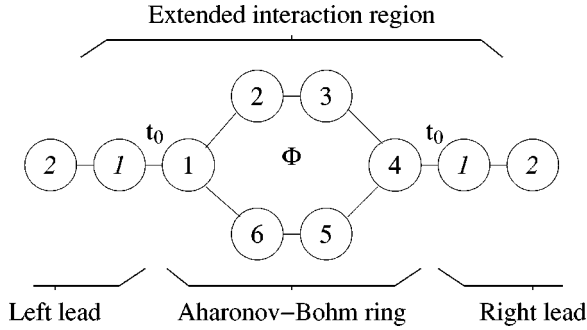


FIG. 1. Aharonov-Bohm ring. Magnetic flux penetrates the center of the ring.

tion in certain cases leads to finite transmission of the incident electron, despite the fact that the total wave function for the scattering electron and electrons bound on the AB ring preserves full quantum coherence. We will therefore refer to the processes that lead to finite transmission in the case where  $\Phi = \pi$  as *dephasing* processes since they clearly lead to diminished AB oscillations observed in experiments. We show that dephasing can occur either by (a) inelastic processes where the tunneling electron excites bound electrons on the ring or by (b) elastic (in regard to energy) processes, where the tunneling electron changes the symmetry or the spin of the degenerate many-electron wave function. No exchange of energy is required in the latter case:<sup>19–22</sup> dephasing occurs because the tunneling electron leaves a trace on its “environment,” which consists of bound electrons.

## II. METHOD

The proposed method is based on the multichannel scattering technique that was developed for studying the tunneling of a single electron in the presence of scattering by phonons.<sup>23,24</sup> Since its introduction, it has been successfully applied to a variety of problems where a single electron is coupled to phonon modes.<sup>4,25–31</sup> It was even incorporated into Landauer theory where the influence of electron-phonon scattering on the nonequilibrium electron distribution has been investigated.<sup>32</sup> We now generalize this method to study many-electron problems.

### A. Model Hamiltonian

While the method can be applied to more general situations and arbitrary geometries of the interaction region, we choose for simplicity a particular physical system which will also serve as a toy model for the study of the  $e$ - $e$  interaction induced dephasing. We thus consider an AB ring coupled to two ideal one-dimensional leads; see Fig. 1. The ring is described by a Hubbard-type Hamiltonian

$$H_{\text{ring}} = \sum_{j,\sigma} (\epsilon c_{j\sigma}^\dagger c_{j,\sigma} - t e^{i\phi_j} c_{j+1,\sigma}^\dagger c_{j,\sigma} + \text{H.c.}) + U \sum_j c_{j,\uparrow}^\dagger c_{j,\uparrow} c_{j,\downarrow}^\dagger c_{j,\downarrow}. \quad (1)$$

The operator  $c_{j\sigma}^\dagger$  creates an electron with spin  $\sigma$  at site  $j$  and we make a formal identification  $c_{7,\sigma}^\dagger = c_{1,\sigma}^\dagger$ . The phases  $\phi_j$  describe phase changes due to magnetic flux penetrating the ring. We chose a gauge in which we ascribe the total phase change due to magnetic-field flux,  $\Phi = 2\pi\Phi_M/\Phi_0$  (where  $\Phi_M$  is the magnetic field flux and  $\Phi_0 = h/e$  is the flux quantum), to a single element, e.g.,  $\phi_1 = \Phi$  and  $\phi_j = 0$  ( $j \neq 1$ ).

The leads are described by a tight-binding Hamiltonian

$$H_{\text{lead}} = -t_{\text{lead}} \sum_{i,\sigma} a_{i+1,\sigma}^\dagger a_{i,\sigma} + \text{H.c.} \quad (2)$$

$$-t_{\text{lead}} \sum_{i,\sigma} b_{i+1,\sigma}^\dagger b_{i,\sigma} + \text{H.c.} \quad (3)$$

The operator  $a_{i,\sigma}^\dagger$  creates an electron with spin  $\sigma$  at site  $i$  on the left lead, while the operator  $b_{i,\sigma}^\dagger$  does the same on the right lead. The ring is coupled to the electrodes with coupling constants  $t_0$ ,

$$H_c = -t_0 \sum_{\sigma} (a_{1,\sigma}^\dagger c_{1,\sigma} + \text{H.c.}) - t_0 \sum_{\sigma} (b_{1,\sigma}^\dagger c_{4,\sigma} + \text{H.c.}). \quad (4)$$

The coupling constant  $t_0$  need not be small: the method applies equally well for strong coupling between the interaction region and the leads.

### B. Correlated many-electron states and exact diagonalization

The transmittivity can be meaningfully defined in a many-electron scattering problem only if one single electron leaves the scattering region. For this reason, we restrict the energy of the incoming electron to be below the ionization threshold. Our approximation then consists of taking into account only those many-electron states in which at most one (scattering) electron is located outside the ring. Before the impact of the electron (which, for convenience, will be chosen to have spin up), there are  $n = n_\uparrow + n_\downarrow$  other electrons bound on the AB ring. We truncate all many-body states, where additional electrons hop from the interacting region to the lead. When physical parameters of the system, e.g. ( $\epsilon, t, U$ ), are chosen in such a way that these  $n$  electrons are bound in the interacting region, the approximation is equivalent to neglecting the exponentially decaying tails of the  $n$ -electron wave function in the leads.

Before the scattering, the bound electrons are therefore in one of the  $n$ -particle eigenstates of the Hamiltonian  $H_{\text{ring}}$ , Eq. (1). We denote these states by  $|\alpha_i^\uparrow\rangle$  and their energies by  $\epsilon_i^\uparrow$ . The superscript index  $\uparrow$  denotes that the electron in the lead has spin up.

When the incoming electron enters the ring, the system is in a superposition of the  $(n+1)$ -particle states which we denote by  $|\beta_i\rangle$ . These states are not necessarily eigenstates of  $H_{\text{ring}}$ . After the scattering there is a single electron in the leads, while the ring is in a superposition of the  $n$ -particle eigenstates of  $H_{\text{ring}}$ . These states are the  $|\alpha_i^\uparrow\rangle$  states and (in the case where the spin of the scattering electron is flipped)

the  $n$ -electron eigenstates with  $n_{\uparrow} + 1$  spin-up electrons and  $n_{\downarrow} - 1$  spin-down electrons. These spin-flipped states are labeled by  $|\alpha_i^{\downarrow}\rangle$  and their energies by  $\epsilon_i^{\downarrow}$ . Because all the possible states of the ring after scattering are orthogonal to each other, the outgoing channels are well defined and the current is conserved.

We calculate the eigenstates  $|\alpha_i^{\sigma}\rangle$  using exact diagonalization of the Hamiltonian  $H_{\text{ring}}$  in the suitable region of the many-particle Hilbert space, taking into account that the Hubbard Hamiltonian is invariant with respect to rotations in the spin space. The diagonalization is therefore performed in the constant  $(n, S_z)$  space, where  $S_z$  is the conserved component of the total spin in the  $z$  direction. The method can be applied to Hamiltonians that do not conserve  $S_z$  at the expense of significantly more time consuming numerical calculations.

At zero temperature, the electron scatters on the ground state of the  $n$ -particle state in the ring,  $|\alpha_0^{\uparrow}\rangle$ . During the scattering the electron can loose energy by exciting the bound electrons into one of the excited  $|\alpha_i^{\sigma}\rangle$  states. The probability of such transitions is a rapidly decreasing function of the energy loss, therefore only a small number of the scattering channels (states  $|\alpha_i^{\sigma}\rangle$ ) has to be considered. This observation is essential for numerical performance of the method: we can efficiently calculate the states from the bottom of the spectrum of the matrix representations of  $H$  in suitable  $(n, S_z)$  subspaces using the iterative Lanczos technique. We have used the implicitly restarted Lanczos method, as implemented in ARPACK package.<sup>33</sup> The eigenvalues and eigenvectors were computed to machine precision.

By taking into account only the allowed states, the wave function that describes the scattering of one electron on the AB ring is given by

$$|\Psi\rangle = \sum_{i=1}^{\infty} \sum_{j,\sigma} d_{i,j,\sigma}^L a_{i,\sigma}^{\dagger} |\alpha_j^{\sigma}\rangle + \sum_{i=1}^{\infty} \sum_{j,\sigma} d_{i,j,\sigma}^R b_{i,\sigma}^{\dagger} |\alpha_j^{\sigma}\rangle + \sum_j e_j |\beta_j\rangle, \quad (5)$$

where  $d_{i,j,\sigma}^L$ ,  $d_{i,j,\sigma}^R$ , and  $e_k$  are the coefficients to be determined.

### C. Reduction to a sparse system of linear equations

We consider a steady-state scattering described by the Schrödinger equation

$$H|\Psi\rangle = E|\Psi\rangle, \quad (6)$$

with  $H = H_{\text{ring}} + H_{\text{lead}} + H_c$ . This equation cannot be exactly solved in the space, spanned on the  $|\alpha_i^{\sigma}\rangle$  and  $|\beta_j\rangle$  states, because applying the Hamiltonian to the wave-function ansatz takes us out of this space by generating terms where more than one electron exits the scattering region. Omission of these terms represents the main approximation used in our method. This approximation leads to an error that is not significant for suitably chosen model parameters (see below).

Operating on Eq. (6) from the left with  $\langle\beta_l|$ , we obtain

$$-t_0 \sum_{j,\sigma} b_{l,j,\sigma}^L d_{1,j,\sigma}^L - t_0 \sum_{j,\sigma} b_{l,j,\sigma}^R d_{1,j,\sigma}^R + \sum_k h_{l,k} e_k = E e_l, \quad (7)$$

where  $b$ 's denote scalar products

$$b_{l,j,\sigma}^L = \langle\beta_l|c_{1,\sigma}^{\dagger}|\alpha_j^{\sigma}\rangle, \\ b_{l,j,\sigma}^R = \langle\beta_l|c_{4,\sigma}^{\dagger}|\alpha_j^{\sigma}\rangle, \quad (8)$$

while  $h_{l,k} = \langle\beta_l|H_{\text{ring}}|\beta_k\rangle$  are the matrix elements of Hamiltonian  $H_{\text{ring}}$  in the  $n+1$  electron subspace.

By operating with  $\langle\alpha_j^{\sigma}|a_{1,\sigma}$  from the left we get

$$-t_{\text{lead}} d_{2,j,\sigma}^L - t_0 \sum_k (b_{k,j,\sigma}^L)^* e_k + \epsilon_j^{\sigma} d_{1,j,\sigma}^L = E d_{1,j,\sigma}^L. \quad (9)$$

### D. Pruning the leads

In an open outgoing channel  $(j, \sigma)$  a plane wave can propagate, so that  $d_{2,j,\sigma}^L = \exp(ik_{j,\sigma}) d_{1,j,\sigma}^L$ . By energy conservation the wave number  $k_{j,\sigma}$  is obtained from

$$\epsilon_0 - 2t_{\text{lead}} \cos(K) = \epsilon_j^{\sigma} - 2t_{\text{lead}} \cos(k_{j,\sigma}). \quad (10)$$

The energy  $\epsilon_0$  is the initial energy of the  $n$ -electron bound state on the ring,  $K$  is the wave number of the incoming electron, and  $\epsilon_j^{\sigma}$  is the final energy of the bound electrons. Equation (9) can thus be written as

$$d_{1,j,\sigma}^L = \frac{-t_0 \sum_k (b_{k,j,\sigma}^L)^* e_k}{E - \epsilon_j^{\sigma} + t_{\text{lead}} \exp(ik_{j,\sigma})}. \quad (11)$$

Similar equation can be obtained for exponentially decaying (closed) outgoing channels that we also take into account (up to some cutoff energy, above which the inclusion of further closed channels does not change the results). These are defined through the relation  $d_{2,j,\sigma}^L = \exp(-\kappa_{j,\sigma}) d_{1,j,\sigma}^L$  and

$$\epsilon_0 - 2t_{\text{lead}} \cos(K) = \epsilon_j^{\sigma} - 2t_{\text{lead}} \cosh(k_{j,\sigma}). \quad (12)$$

Equation (9) can, in this case, be written as

$$d_{1,j,\sigma}^L = \frac{-t_0 \sum_k (b_{k,j,\sigma}^L)^* e_k}{E - \epsilon_j^{\sigma} + t_{\text{lead}} \exp(-\kappa_{j,\sigma})}. \quad (13)$$

In the incoming channel we have both the incoming and outgoing waves,  $d_{m,0,\uparrow}^L = \exp(-iKm) + r \exp(iKm)$ . We obtain  $d_{2,0,\uparrow}^L = \exp(iK) d_{1,0,\uparrow}^L + \exp(-2iK) - 1$ . The equation for the incoming channel thus contains an additional inhomogeneous term  $\exp(-2iK) - 1$ , and Eq. (9) for the incoming channel is

$$d_{1,0,\uparrow}^L = \frac{-t_0 \sum_k (b_{k,0,\uparrow}^L)^* e_k - t_{\text{lead}} [\exp(-2iK) - 1]}{E - \epsilon_0 + t_{\text{lead}} \exp(iK)}. \quad (14)$$

Using Eqs. (11), (13), and (14), and similar equations for the right lead, both leads can be removed (pruned) from the problem.<sup>24</sup>

Equations (7), (11) and equivalent equations for other outgoing channels form a system of linear equations for unknowns  $d_{1,j,\sigma}^L$ ,  $d_{1,j,\sigma}^R$ , and  $e_j$ . This sparse system is solved for different energies of the incoming electron using the SuperLU library.<sup>34</sup>

The partial transmittivity through channel  $(j, \sigma)$  is given by

$$T_{j,\sigma}(E) = \frac{\sin(k_{j,\sigma})}{\sin(K)} |d_{1,j,\sigma}^R|^2. \quad (15)$$

Since the method is based on exact solution of many-electron problem, we can compute transmission at arbitrarily large values of  $U$ .

### E. Extended interaction region

Results can be improved by extending the interaction region which is solved exactly by the Lanczos method by adding additional sites from the leads. This procedure takes into account the decaying tails of bound electron wave functions in the leads at the expense of increasing the computational Hilbert space. The error due to the omission of the terms corresponding to a second electron jumping out of the original interaction region [see discussion following Eq. (6)] is exponentially reduced with the inclusion of each additional site from the leads.

These improvements mainly lead to energy shifts of the resonance peaks while the general characteristics of the spectra remain unchanged. In principle, the region could be extended until the desired convergence is achieved. In our calculations the interacting region consisted of the ring and one additional site from each lead; see Fig. 1. In fact, we had to take into account the site on the left electrode in order to ensure that the incident electron spreads into two partial waves that propagate through both arms of the ring. The additional site on the right electrode is required so that the partial waves can interfere, which leads to the proper description of the Aharonov-Bohm effect. The inclusion of these two sites was therefore essential in our studies of the dephasing mechanisms.

In cases where the ground state of the interaction region was degenerate, we averaged the transmittivity spectra over all the degenerate states. The variational space taken into account in our calculation was equivalent to a Hubbard model on eight sites with no translational symmetry.

The largest problem that could be effectively solved has three bound electrons with spin up and four electrons with spin down. In this case there are  $\sim 8000$   $|\alpha_i^\sigma\rangle$  states and  $\sim 5000$   $|\beta_i\rangle$  states. We kept 200 lowest-lying  $|\alpha_i^\sigma\rangle$  states to define our scattering channels (diagonalization took 3 min of a modest personal computer). Solving the sparse system of complex linear equations for a range of the incoming electron energies took 200 min for 237 data points (or about 1 min per data point on the average). This step is the most computationally demanding part of our technique. This is the

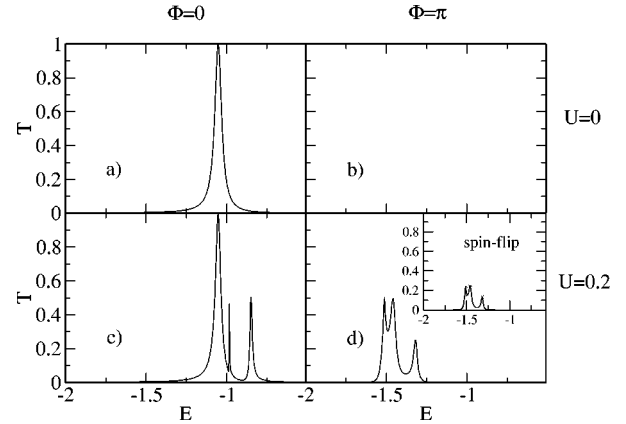


FIG. 2. Transmission probability as a function of the incident electron energy for one electron with spin down bound on the ring. The incoming electron had spin up. The coupling to the lead is  $t_0 = 0.4$ . In all cases transmission is purely elastic.

main reason why we limited our calculations to eight site models, even though the Lanczos method easily handles much larger lattices.

### III. RESULTS—ONE BOUND ELECTRON

We now investigate the effect of interactions on an electron as it tunnels through the ring. The incoming electron has spin up, and there is one bound electron with spin down inside the ring. The on-site energies are  $\epsilon = -4.5t_{\text{lead}}$ , the overlap integrals are  $t = \sqrt{3}t_{\text{lead}}$ , and we set  $t_{\text{lead}} = 1$ .

First we consider the noninteracting case. In the absence of the magnetic field the transmission reaches unity at the resonance, Fig. 2(a). The electron is fully reflected at any incident energy when the magnetic flux is  $\Phi = \pi$ , Fig. 2(b). This is the usual Aharonov-Bohm effect.

We now turn on the interaction. At  $\Phi = 0$ , we still see a unity peak at the energy of the single-electron resonance, followed by smaller satellite peaks caused by the interaction, Fig. 2(c). At  $\Phi = \pi$ , when in the absence of  $U$  the electron is fully reflected, we obtain very high transmission probability despite relatively small  $U = 0.2$ , Fig. 2(d). In the largest peak the transmission approaches the value  $T = 1/2$ . Since the incoming electron and the bound electron are not entangled, their total spin is not well defined, therefore the total wave function is a superposition of a singlet and a triplet state with equal amplitudes:  $|\uparrow\downarrow\rangle = 1/\sqrt{2}(|S=1, S_z=0\rangle + |S=0, S_z=0\rangle)$ . The triplet scattering has zero transmission probability at  $\Phi = \pi$  since in the Hubbard model only singlet electrons interact. The singlet scattering, however, reaches the unitary limit at the main resonance peak. Averaging over both contributions, we indeed get  $T = 1/2$ .

The spin-flip scattering part of the transmission probability is shown in the inset of Fig. 2(d). The spin-flip and normal scattering contribute equally to the total transmission probability. Both are purely elastic with respect to energy changes.

### A. Lead decoupling at $\Phi = \pi$ and scattering mechanisms at nonzero $U$

To gain more insight into the mechanism of nonzero electron tunneling probability, we present a simple physical picture of electron tunneling for the case of  $\Phi = \pi$ . We first transform the AB ring Hamiltonian (1) from the basis of localized states to a basis in  $k$  space. For more generality, we can now assume that the ring consists of an arbitrary even number  $m$  of sites, which we now number from 0 to  $m-1$ , so that site 0 is coupled to the left electrode, while site  $m/2$  is coupled to the right electrode.

The noninteracting part of the Hamiltonian (1) is diagonal in the plane-wave basis,

$$d_{n,\sigma} = \frac{1}{\sqrt{m}} \sum_{j=1}^m e^{-ijk_n} c_{j,\sigma}, \quad (16)$$

with wave numbers  $k_n$  given by the periodic boundary condition  $\exp(ik_n m) = 1$ , or  $k_n = 2\pi n/m$ , where  $n = 0, \pm 1, \dots, \pm m/2 - 1, m/2$ . The corresponding eigenvalues are

$$E_n = \epsilon - 2t \cos(k_n - \Phi/m). \quad (17)$$

When  $\Phi = \pi$ , all the noninteracting eigenstates are twofold degenerate since  $\cos[k_n - (\pi/m)] = \cos[k_{1-n} - (\pi/m)]$ . The complete orthonormal set of states is therefore composed of  $m/2$  pairs of states with wave numbers  $k_n$  and  $k_{1-n}$  for  $n$  ranging from 1 to  $m/2$ . For each pair we can form two linear combinations of states:

$$\begin{aligned} a_{L,n,\sigma} &= \frac{1}{\sqrt{2}} (d_{n,\sigma} + d_{1-n,\sigma}) \\ &= \frac{1}{\sqrt{2m}} \sum_j (e^{ik_n j} + e^{-ik_n j} e^{i2\pi j/m}) c_{j,\sigma}, \\ a_{R,n,\sigma} &= \frac{1}{\sqrt{2}} (d_{n,\sigma} - d_{1-n,\sigma}) \\ &= \frac{1}{\sqrt{2m}} \sum_j (e^{ik_n j} - e^{-ik_n j} e^{i2\pi j/m}) c_{j,\sigma}. \end{aligned} \quad (18)$$

It is easy to see that the coefficient of  $c_{m/2,\sigma}$  in the expression for  $a_{L,n,\sigma}$  is zero, and likewise for the coefficient of  $c_{0,\sigma}$  in the expression for  $a_{R,n,\sigma}$ . This means that the eigenstate denoted by  $L$  is coupled only to the left electrode, while eigenstate  $R$  is coupled only to the right electrode; see Fig. 3. In the noninteracting case the incoming electron can only tunnel from the left electrode to an  $L$  state. This state is decoupled from the right electrode, and since there is no term in the Hamiltonian, which would allow transitions from  $L$  to  $R$  state, the electron is fully reflected.

There are therefore two equivalent physical descriptions of zero transmittivity of an AB ring. One can either consider it as a destructive interference of partial electron waves that

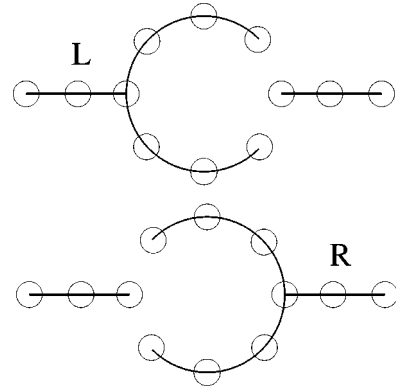


FIG. 3. At  $\Phi = \pi$ , one can rotate each pair of the degenerate eigenstates in such a way that one of them couples only to the left electrode and the other to the right electrode. In the absence of interactions both electrodes are effectively decoupled.

travel in the upper and lower arm of the ring, or as an effective decoupling of both electrodes due to a topological phase shift.

We will now write the interacting part of the Hamiltonian in the new basis and search for processes that are responsible for the nonzero transmission. From Eqs. (16) and (18) we can express  $c_{j,\sigma}$  as

$$c_{j,\sigma} = \frac{2e^{i(\pi j/m)}}{\sqrt{2m}} \sum_{n=1}^{m/2} [\cos(\tilde{k}_n j) a_{L,n,\sigma} + \sin(\tilde{k}_n j) a_{R,n,\sigma}], \quad (19)$$

where we have introduced shifted wave numbers

$$\tilde{k}_n = \frac{2\pi}{m} \left( n - \frac{1}{2} \right). \quad (20)$$

The particle number operator can then be expressed as

$$\begin{aligned} c_{j,\sigma}^\dagger c_{j,\sigma} &= \frac{2}{m} \sum_{p,q} \cos(\tilde{k}_p j) \cos(\tilde{k}_q j) a_{L,p,\sigma}^\dagger a_{L,q,\sigma} \\ &\quad + \sin(\tilde{k}_p j) \sin(\tilde{k}_q j) a_{R,p,\sigma}^\dagger a_{R,q,\sigma} \\ &\quad + \cos(\tilde{k}_p j) \sin(\tilde{k}_q j) a_{L,p,\sigma}^\dagger a_{R,q,\sigma} \\ &\quad + \sin(\tilde{k}_p j) \cos(\tilde{k}_q j) a_{R,p,\sigma}^\dagger a_{L,q,\sigma}. \end{aligned} \quad (21)$$

We now see that the Hubbard interaction term  $\sum_j c_{j,\uparrow}^\dagger c_{j,\uparrow} c_{j,\downarrow}^\dagger c_{j,\downarrow}$  is a sum over  $j$  of products of four trigonometric functions. Each one of these products can be written as a sum of trigonometric functions by using trigonometric reduction formulas such as,

$$\begin{aligned} &8 \sin(a) \sin(b) \sin(c) \sin(d) \\ &= -\cos(a-b-c-d) + \cos(a+b-c-d) \\ &\quad + \cos(a-b+c-d) - \cos(a+b+c-d) \\ &\quad + \cos(a-b-c+d) - \cos(a+b-c+d) \\ &\quad - \cos(a-b+c+d) + \cos(a+b+c+d). \end{aligned} \quad (22)$$

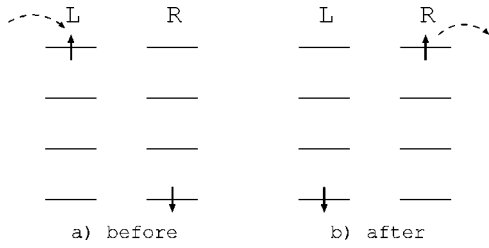


FIG. 4. Transmission due to elastic symmetry-changing scattering.

We note that reduction formulas for an even number of sine and cosine functions consist of a sum of cosine functions, while the reduction formulas for an odd number of sine and cosine functions consist of a sum of sine functions. This fact is important to understand the selection rules that lead to dephasing.

The arguments of functions on the right-hand sides of the reduction formulas are sums of the form

$$\frac{2\pi j}{m} \left[ p - \frac{1}{2} \pm \left( q - \frac{1}{2} \right) \pm \left( r - \frac{1}{2} \right) \pm \left( s - \frac{1}{2} \right) \right],$$

i.e., of form  $2\pi jt/m$ , where  $t$  is an integer. When the summation over site index  $j$  is performed, most of the terms will drop, since

$$\begin{aligned} \frac{1}{m} \sum_{j=1}^m \cos\left(\frac{2\pi t}{m} j\right) &= \delta_{t,0}, \\ \frac{1}{m} \sum_{j=1}^m \sin\left(\frac{2\pi t}{m} j\right) &= 0, \end{aligned} \quad (23)$$

where the first line in Eq. (23) can also be viewed as the momentum conservation for the case of twisted boundary conditions. All interaction terms with a coefficient that after trigonometric reduction involves a sine function will therefore vanish. Such vanishing terms come from products of an odd number of trigonometric functions of each kind, therefore they are of the form such as

$$a_{R,p,\uparrow}^\dagger a_{L,q,\uparrow} a_{L,r,\downarrow}^\dagger a_{L,s,\downarrow}. \quad (24)$$

Such terms would allow (for  $p=q, r=s$ ) transitions of the tunneling electron from state  $L$  to  $R$  without changing the bound-electron state (i.e., without leaving any imprint on the environment). Such transitions would clearly be in contradiction with our understanding of the dephasing in the AB rings.

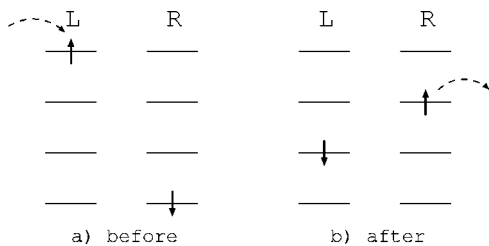


FIG. 5. Transmission due to inelastic symmetry-changing scattering.

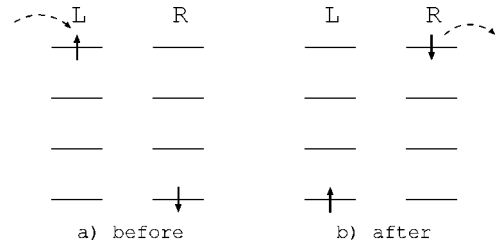


FIG. 6. Transmission due to elastic spin-flip scattering.

The terms with four sine and with four cosine functions are of little importance for our purposes. They describe interlevel repulsion and interlevel transitions without changes of the  $LR$  character of the electron states, and therefore do not lead to a finite transmission. We will focus instead on terms with two sine and two cosine functions. They are of three kinds. The first one consists of terms of the form

$$a_{R,p,\uparrow}^\dagger a_{L,q,\uparrow} a_{L,r,\downarrow}^\dagger a_{R,s,\downarrow}. \quad (25)$$

These terms describe what we call *symmetry-changing transitions*: the tunneling electron (with spin up) in the  $L$  state jumps to a  $R$  state, while a bound electron undergoes a transition from  $R$  to  $L$  state. Such a transition can either be elastic (with respect to the energy of the tunneling electron) if  $p=q, r=s$  (Fig. 4), or inelastic (Fig. 5). The second kind of terms is of the form

$$a_{L,p,\uparrow}^\dagger a_{L,q,\uparrow} a_{R,r,\downarrow}^\dagger a_{R,s,\downarrow}. \quad (26)$$

These terms correspond to *spin-flip transitions*: the tunneling electron with spin up in the  $L, q$  state makes a transition to a lower-laying  $L, p$  state, while a bound electron undergoes a transition from the  $R, s$  to the  $R, r$  state, Fig. 6. Transition can again be either elastic (with respect to energy) for  $p=q, r=s$  (Fig. 6), or inelastic (Fig. 7).

Finally, terms of the form

$$a_{R,p,\uparrow}^\dagger a_{L,q,\uparrow} a_{R,r,\downarrow}^\dagger a_{L,s,\downarrow} \quad (27)$$

can correspond either to symmetry-changing (Fig. 8) or to spin-flip transitions (Fig. 9), depending on the  $p, q, r, s$  quantum numbers.

## B. Scattering of a wave packet

To illustrate more in detail our results presented in the preceding section, we present here numerically exact calculation of scattering of an incoming electron (described as a wave packet with a given finite-energy width) on the electron

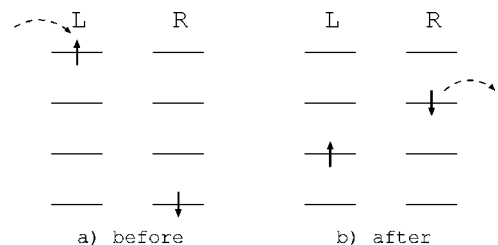


FIG. 7. Transmission due to inelastic spin-flip scattering.

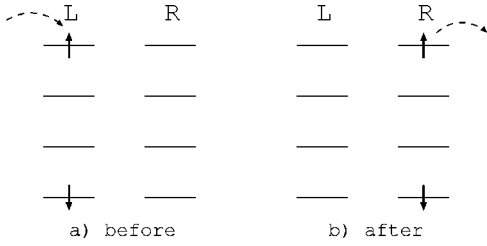


FIG. 8. Transmission due to elastic symmetry-changing scattering (of the second kind).

with the opposite spin, bound on the Aharonov-Bohm ring. Since we are dealing with a simple case of only two electrons, this problem can be solved numerically exactly by direct integration of the two-body Schrödinger equation  $i\hbar d|\psi\rangle/dt = H|\psi\rangle$ . We take into consideration a sufficiently high number of chain sites, so that the positional spread of the wave packet is smaller than the length of the left and the right lead. We choose  $N=200$  sites, where the six-site Aharonov-Bohm ring occupies positions ranging from 101 to 106.

We construct the wave function at the initial time as  $|\psi\rangle = \psi_{\uparrow\text{packet}}^\dagger \phi_{\downarrow\text{bound}}^\dagger |0\rangle$ . The operator  $\phi_{\downarrow\text{bound}}^\dagger$  creates an electron with spin down in the bound eigenstate of the Aharonov-Bohm ring. We calculated this state using direct diagonalization. The operator  $\psi_{\uparrow\text{packet}}^\dagger$  is

$$\psi_{\uparrow\text{packet}}^\dagger = C \sum_k \exp\left[-\frac{(k-k_0)^2}{2\sigma^2}\right] \exp(-ikN_{\text{center}}) c_{\uparrow k}^\dagger, \quad (28)$$

where  $c_{\uparrow k}^\dagger = 1/\sqrt{N} \sum_{j=1}^N \exp(ikj) c_{\uparrow j}^\dagger$  and  $C$  is a normalization constant. This operator creates an electron with spin up in a wave packet centered at site  $N_{\text{center}}$ , which has the average wave number  $k_0$  and a spread of  $\sigma$  in the  $k$  space. We choose  $k_0 = \pi/2$  to place the wave packet in the middle of the energy band of the leads with the group velocity  $v = \partial E / \partial k(k=k_0) = t = 1$ . We set  $\sigma = 0.13$  and  $N_{\text{center}} = 50$ .

The equation of motion was then integrated using Bulirsch-Stoer method, which gives highly accurate results for this type of problem. The accuracy and stability can be conveniently estimated by monitoring the deviation from the proper normalization of the wave-function. Using the Bulirsch-Stoer method, the normalization differs from 1 at the eighth decimal place after the scattering.

We set the parameters to  $\epsilon = -3.0$ ,  $t = \sqrt{3}$ ,  $t_0 = 0.6$ , and  $t_{\text{lead}} = 1$ . For the noninteracting system the transmittivity at

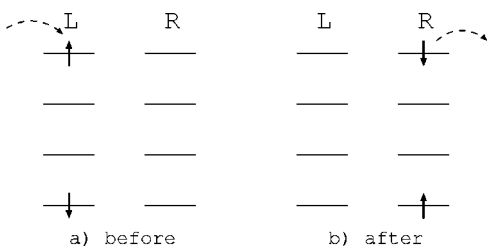


FIG. 9. Transmission due to elastic spin-flip scattering (of the second kind).

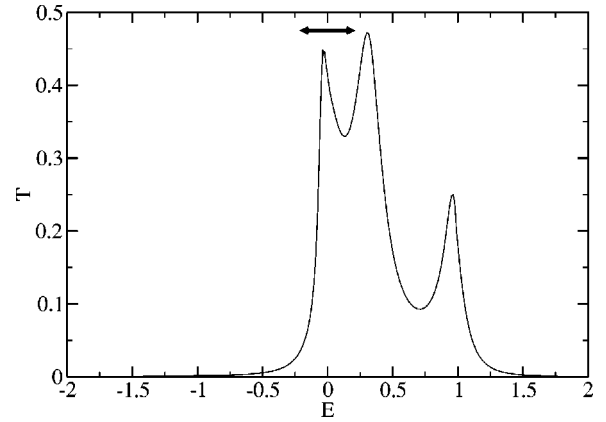


FIG. 10. Transmission probability as a function of the incident electron energy for one electron with spin down bound on the ring.

$\Phi = \pi$  is 0 for all electron energies, while the transmittivity of an interacting system with  $U=1$  is shown in Fig. 10. The location and the spread of the energies of the wave packet are represented in the figure by a two-sided arrow.

The electron density before and after the scattering at  $\Phi = \pi$  is shown in Fig. 11 for the noninteracting case and in Fig. 12 for the interacting case.<sup>37</sup> For  $U=0$ , the wave packet is perfectly reflected, as expected. For  $U=1$ , the wave packet is partially transmitted through the scattering region. In fact, the expectation value to find an electron in the second electrode,  $P_R$ , corresponds to the following average:

$$P_R = \int dk T[\epsilon(k)] |\psi_{\uparrow\text{packet}}^\dagger(k, t=0)|^2, \quad (29)$$

where the transmission  $T$  is calculated using the method from Sec. II and is presented in Fig. 10. This equation connects and thus validates the two distinct methods. It is furthermore worth stressing that the probability of finding electrons with either orientation of spin in the second electrode is equal; see

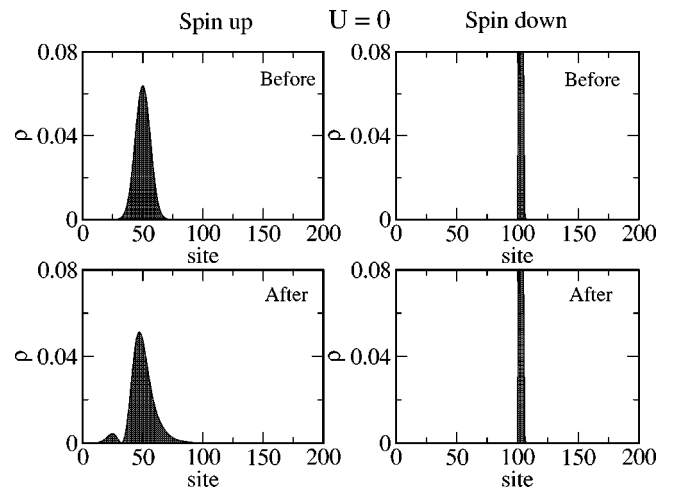


FIG. 11. Electron density before and after the scattering of the wave packet on an Aharonov-Bohm ring at  $\Phi = \pi$ : noninteracting case. Note that the vertical scale is the same for both spin projections: the scale was chosen so that the wave packet is clearly visible.

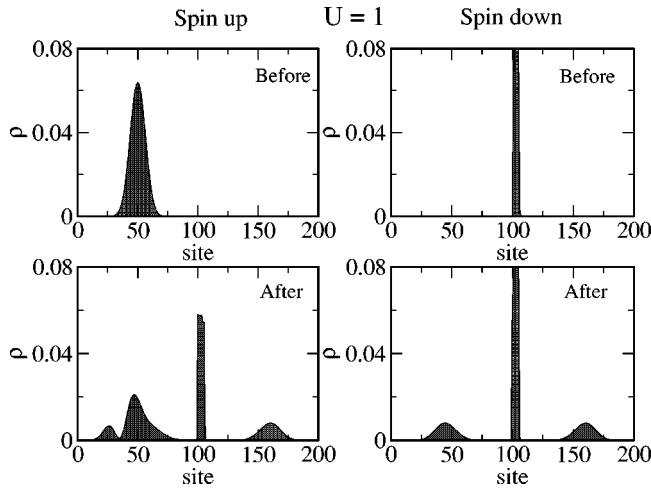


FIG. 12. Electron density before and after the scattering of the wave packet on the Aharonov-Bohm ring at  $\Phi = \pi$ : interacting case.

Figs. 12 and 13. This can be explained as follows: finite transmission is a direct consequence of interaction  $U$ , which in the case of two electrons acts only on the singlet part of the wave function. The triplet part does not feel  $U$  due to the on-site nature of the interaction. Transmission therefore occurs only through the singlet channel.

### C. Aharonov-Bohm oscillations

Aharonov-Bohm effect is experimentally observed as magnetic-flux-dependent oscillations of the electric current through a mesoscopic ring structure.<sup>1</sup> From calculated  $T(E)$  spectra we could estimate the zero-bias conductance as  $G = G_0 T(E_F)$ , where  $G_0 = 2e^2/h$  is the conductance quantum and  $E_F$  is the common Fermi level of both leads. In our minimal model with a discrete number of resonance states in the ring, the energy shifts of the peaks when the flux is changed [see Eq. (17)] lead to pronounced conductance variations not necessarily connected to the Aharonov-Bohm effect itself. This is a direct consequence of using a small

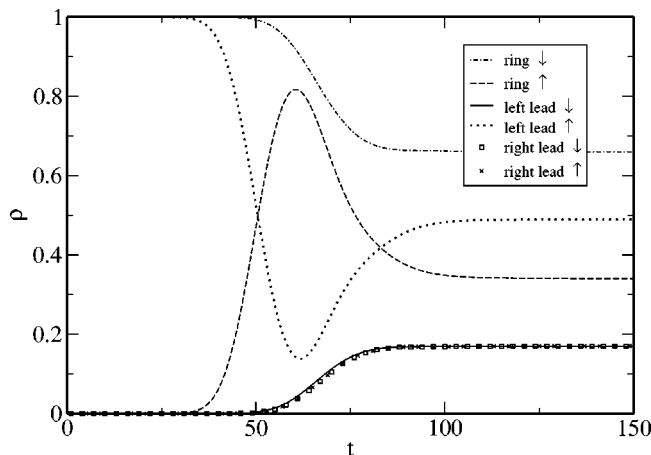


FIG. 13. Time dependence (for interacting case) of the probability to find an electron with given spin projection either in the ring, in the left electrode, or in the right electrode.

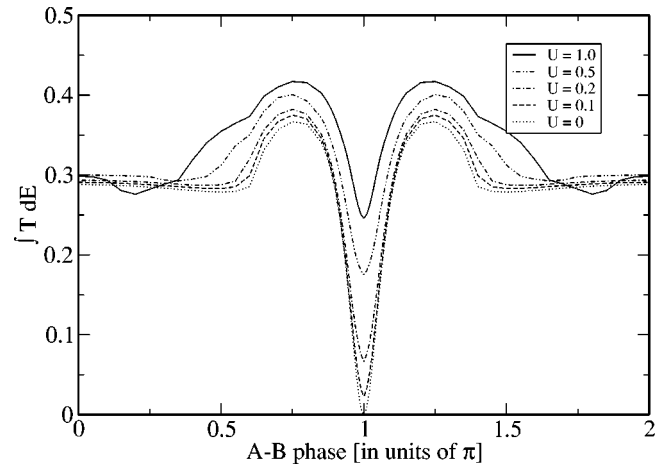


FIG. 14. The flux dependence of integrated transmission probability for different interaction strengths. The coupling to the leads is  $t_0 = 0.6$ , all other parameters are as before.

discrete number of sites. It is therefore more revealing to observe the variations of the *integral* of transmittivity over the whole energy band,  $\int T(E) dE$ . This quantity is relatively insensitive to energy shifts of the peaks, while it should clearly show AB oscillations which affect the height of all of the peaks.

In Fig. 14 we present this integral as a function of  $\Phi$  for a number of increasing interaction strengths  $U = 0, 0.1, \dots, 1.0$ . The amplitude of AB oscillations noticeably decreases as the interaction grows stronger. Figure 14 also shows that the integral transmittivity is essentially interaction independent around zero flux,  $\Phi = 0$ . A similar insensitivity of the transmittivity sum rule has been discovered in the case of tunneling in the presence of electron-phonon coupling.<sup>4,35,36</sup> This insensitivity breaks down at larger  $U$ .

### IV. MANY BOUND ELECTRONS ON THE RING

We now consider several interacting ( $U = 1$ ) bound electrons on the ring. All presented cases are calculated at the flux value  $\Phi = \pi$ , unless otherwise specified. Spin of the incoming electron is up. We have limited the energy of the incident electron to a half of the bandwidth, i.e.,  $E = [-2, 0]$ , in order to avoid ionization. Our main goal in this section is to investigate the circumstances under which a scattering electron obtains a finite transmission probability at  $\Phi = \pi$  when scattering through the AB ring in the presence of many bound electrons. We show that in most cases Coulomb interaction leads to finite transmission. In our work we refer to processes that cause finite transmission as *dephasing processes*. To avoid confusion we point out once more that the total wave function describing a many-body state of the scattering electron and bound electrons preserves its full quantum coherence throughout the calculation. Our Hamiltonian does not contain coupling to external degrees of freedom, that would naturally lead to dephasing.

When the bound state on the ring consists of three electrons with spin up and one electron with spin down [Fig. 15(a)], no spin-flip scattering is possible because such pro-

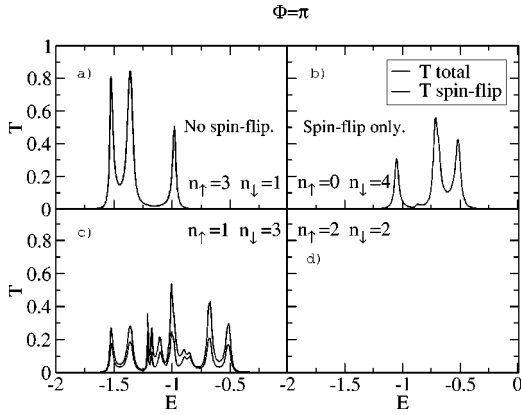


FIG. 15. Transmission probability as a function of the incident electron energy for  $n_{\uparrow}$  ( $n_{\downarrow}$ ) electrons with spin up (down). Parameters are  $\epsilon = -4.5$ ,  $t = \sqrt{3}$ ,  $U = 1.0$ ,  $t_0 = 0.3$ , and  $t_{\text{lead}} = 1$ .

cesses turn out to be energetically impossible. The ground state is, however, fourfold degenerate and the tunneling electron can get through the ring at finite  $U$  by changing the symmetry of the many-electron state on the ring. Since the ground state is degenerate, this process is purely elastic.

In the case of  $n_{\uparrow} = 0, n_{\downarrow} = 4$  [Fig. 15(b)], the ground state is nondegenerate, however, the spin-flip processes are energetically allowed. We therefore obtain transmission probability only in spin-flipped channels. Since in this case the ground state is not degenerate, the transmission consists of purely inelastic processes.

In the case where the ground state is degenerate and the spin-flip processes are allowed, we expect dephasing to occur both with or without spin flip. Such is the case of  $n_{\uparrow} = 1, n_{\downarrow} = 3$  [Fig. 15(c)]. The transmittivity without spin flip is purely elastic, while the spin-flip processes are predominantly elastic, with small contribution from inelastic channels.

Finally, for  $n_{\uparrow} = 2, n_{\downarrow} = 2$ , electrons are fully reflected from the ring since there are no allowed scattering channels in the appropriate energy interval, Fig. 15(d).

We finally show the influence of large  $U = 15$  on the case of  $n_{\uparrow} = 2, n_{\downarrow} = 2$ , where at  $U = 1$  transmission remained zero in the whole interval of incoming electron energy due to widely spaced many-electron levels. At large  $U = 15$ , the energy difference between the nondegenerate ground state and the first excited state decreases in comparison with  $U = 1$  case, as the states become compressed in the lower Hubbard band. We changed the on-site energy to  $\epsilon = -20$  in order to keep the electrons bound on the ring. At  $\Phi = 0$ , there are several energies at which the electron can resonantly tunnel through the ring, Fig. 16(a). At  $\Phi = \pi$ , the electron can only tunnel inelastically. The energy difference to the first excited state in the  $n$  electron Hubbard band is approximately 1.4. We indeed find that only the electrons that are more than 1.4 above the bottom of the energy band can tunnel, Fig. 16(b). Such inelastic processes occur both without [Fig. 16(c)] or with spin flip [Fig. 16(d)].

## V. CONCLUSIONS

Using a simple model and an alternative numerical method we have investigated physics of single electron tun-

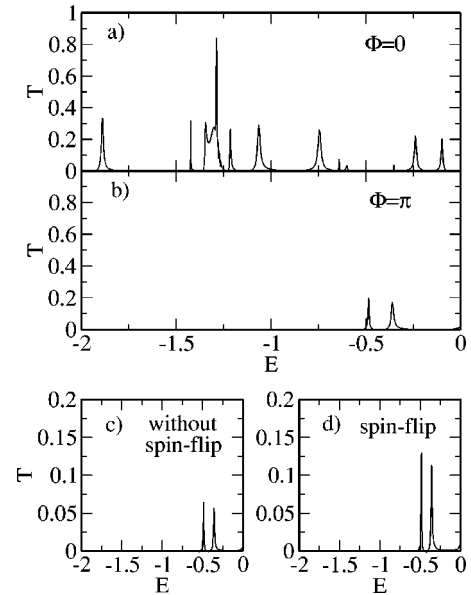


FIG. 16. Transmission probability as a function of incident electron energy for  $n_{\uparrow} = 2, n_{\downarrow} = 2$ ,  $U = 15$ , and  $\epsilon = -20$ .

neling through the AB ring in the presence of correlated bound electrons. In particular, we have focused on the role of electron-electron interactions on dephasing. While the proposed method clearly has some limitations (small interacting regions, inability to describe ionization processes, and neglect of many-body effects in the leads), it nevertheless allows to treat the strong-interaction problem exactly and to identify the two principal microscopic mechanisms that lead to the loss of phase coherence in quantum interference experiments. We showed that a particle can tunnel through the AB ring at  $\Phi = \pi$  elastically by (a) changing the symmetry of the many-electron state, which is possible in the case of degeneracy, or (b) by flipping the spin. Tunneling can also occur in the inelastic channel by exciting the many-electron state on the ring into an excited state with or without the spin flip. Depending on the number of bound electrons, their total spin, degeneracy of the ground state, and available energy of the incoming electron, the total transmission can be composed of partial transmissions caused by either one of the listed processes.

Using the method described here, we have thus unraveled microscopic mechanisms based on electron-electron interaction, which in a mesoscopic system contribute to a finite transmission through the AB ring in the case of  $\Phi = \pi$ . However, since our method is based on small physical systems that can handle only a few lattice sites and interacting electrons, we have no means at this stage to perform accurate calculation of the dephasing rate.

Even though all presented results are obtained on the basis of zero-temperature calculations, the method can be generalized to finite temperatures with some additional numerical effort. On the other hand, our results do not necessarily predict a finite dephasing rate at zero temperature. Since we treat only a single electron in the leads, we are completely neglecting the effects of many-body interactions spreading from the interacting region to the electrons in the leads. This

spread forms the basis for the Kondo effect. At temperatures below the Kondo temperature  $T_K$ , our approach therefore breaks down; in the Kondo regime the spins of the electrons from the interacting region couple into singlets, with the electrons from the leads. This process prevents spin-flip scattering, which in our calculation represents one of the mechanisms for dephasing. Kondo coupling may also lift the degeneracy of the many-electron states in the interacting region, and thus prevent transmission through the elastic channel, which leads to dephasing at zero temperature according to our findings. Other mechanisms leading to dephasing in our approach might as well be modified in this low-temperature regime. We therefore conclude that despite the zero-temperature formalism used in our method, our cal-

culations are relevant only at temperatures higher than the Kondo temperature  $T_K$ .

The method can be applied to study other many-body effects that are expected to be important in nanoscopic structures due to strong electron-electron and electron-phonon coupling. A more general implementation of the presented method is under way.

#### ACKNOWLEDGMENTS

We gratefully acknowledge S. A. Trugman, I. Martin, A. Ramšak, T. Rejec, and J. H. Jefferson for fruitful discussions. The authors also acknowledge the support of the Ministry of Education, Science and Sports of Slovenia.

- 
- <sup>1</sup>R. Webb, S. Washburn, C.P. Umbach, and R.B. Laibowitz, *Phys. Rev. Lett.* **54**, 2696 (1985).  
<sup>2</sup>G. Timp *et al.*, *Phys. Rev. Lett.* **58**, 2814 (1987).  
<sup>3</sup>E. Schuster, E. Buks, M. Heiblum, D. Mahalu, V. Umansky, and H. Shtrikman, *Nature (London)* **385**, 417 (1997).  
<sup>4</sup>K. Haule and J. Bonča, *Phys. Rev. B* **59**, 13087 (1999).  
<sup>5</sup>P. Mohanty, E.M.Q. Jariwala, and R.A. Webb, *Phys. Rev. Lett.* **78**, 3366 (1997).  
<sup>6</sup>P. Mohanty and R.A. Webb, *Phys. Rev. B* **55**, R13452 (1997).  
<sup>7</sup>D. Golubev and A.D. Zaikin, *Phys. Rev. Lett.* **81**, 1074 (1998).  
<sup>8</sup>A.E. Hansen, A. Kristensen, S. Pedersen, C.B. Sorensen, and P. Lindelof, *Phys. Rev. B* **64**, 045324 (2001).  
<sup>9</sup>D. Golubev and A.D. Zaikin, *Phys. Rev. B* **59**, 9195 (1999).  
<sup>10</sup>F. Schopfer, C. Bauerle, W. Rabaud, and L. Saminadayar, *Phys. Rev. Lett.* **90**, 056801 (2003).  
<sup>11</sup>G. Hackenbroich and H.A. Weidenmüller, *Phys. Rev. Lett.* **76**, 110 (1996).  
<sup>12</sup>G. Hackenbroich and H.A. Weidenmüller, *Phys. Rev. B* **53**, 16379 (1996).  
<sup>13</sup>E. Buks, R. Schuster, M. Heiblum, D. Mahalu, V. Umansky, and H. Shtrikman, *Phys. Rev. Lett.* **77**, 4664 (1996).  
<sup>14</sup>W. Hofstetter, J. König, and H. Schoeller, *Phys. Rev. Lett.* **87**, 156803 (2001).  
<sup>15</sup>D. Boese, W. Hofstetter, and H. Schoeller, *Phys. Rev. B* **64**, 125309 (2001).  
<sup>16</sup>B.R. Bulka and P. Stefański, *Phys. Rev. Lett.* **86**, 5128 (2001).  
<sup>17</sup>S. Xiong and Y. Xiong, *Phys. Rev. Lett.* **83**, 1407 (1999).  
<sup>18</sup>O. Entin-Wohlman, A. Aharony, Y. Imry, and Y. Levinson, *Europhys. Lett.* **50**, 354 (2000).  
<sup>19</sup>S.K. Joshi, D. Sahoo, and A.M. Jayannavar, *Phys. Rev. B* **64**, 075320 (2001).  
<sup>20</sup>A. Stern, Y. Aharonov, and Y. Imry, *Phys. Rev. A* **41**, 3436 (1990).  
<sup>21</sup>P.A. Mello, Y. Imry, and B. Shapiro, *Phys. Rev. B* **61**, 16570 (2000).  
<sup>22</sup>J. König and Y. Gefen, *Phys. Rev. B* **65**, 045316 (2002).  
<sup>23</sup>E.V. Anda *et al.*, *Braz. J. Phys.* **24**, 330 (1994).  
<sup>24</sup>J. Bonča and S.A. Trugman, *Phys. Rev. Lett.* **75**, 2566 (1995).  
<sup>25</sup>J. Bonča and S.A. Trugman, *Phys. Rev. Lett.* **79**, 4874 (1997).  
<sup>26</sup>H. Ness and A.J. Fisher, *Phys. Rev. Lett.* **83**, 452 (1999).  
<sup>27</sup>H. Ness, S.A. Shevlin, and A.J. Fisher, *Phys. Rev. B* **63**, 125422 (2001).  
<sup>28</sup>H. Ness and A.J. Fisher, *Europhys. Lett.* **57**, 885 (2002).  
<sup>29</sup>H.M. Pastawski, L.F. Torres, and E. Medina, *Chem. Phys.* **281**, 257 (2002).  
<sup>30</sup>H. Ness and A.J. Fisher, *Chem. Phys.* **281**, 279 (2002).  
<sup>31</sup>L.E.F.F. Torres, H.M. Pastawski, and S.S. Makler, *Phys. Rev. B* **64**, 193304 (2001).  
<sup>32</sup>E.G. Emberly and G. Kirczenow, *Phys. Rev. B* **61**, 5740 (2000).  
<sup>33</sup>R. B. Lehoucq, D. C. Sorensen, and C. Yang, computer code ARPACK (SIAM publishing, Philadelphia, 1997).  
<sup>34</sup>J. W. Demmel, J. R. Gilbert, and X. S. Li, computer code SUPERLU (Lawrence Berkeley National Laboratory, Berkeley, 1999).  
<sup>35</sup>N. Wingreen, K. Jacobsen, and J. Wilkins, *Phys. Rev. Lett.* **61**, 1396 (1988).  
<sup>36</sup>N. Wingreen, K. Jacobsen, and J. Wilkins, *Phys. Rev. B* **40**, 11834 (1989).  
<sup>37</sup>Animations of the scattering process are available upon request from the authors.